UNIVERSITY OF CAMBRIDGE | Energy Policy Research Group

Assessing China's green hydrogen supply and end-use diffusion in hard-to-abate industries

EPRG Working Paper EPRG2404

Cambridge Working Paper in Economics CWPE2426

Haotian Tang, David M. Reiner, Wenying Chen

Abstract

The deep decarbonization of China's hard-to-abate industries requires urgent expansion of clean hydrogen deployment, which is still in its infancy ascribed to its weak cost-competitiveness compared with the fossil-based counterparts and uncertain diffusion prospects. To address this problem, this study evaluates the supply potential and levelized cost of hydrogen production from onshore wind and solar PV on a 1 km-grid level, which collaborates with the established bottom-up plant-level hydrogen demand inventory to reveal the spatial heterogeneity and sectoral disparity of the hydrogen layouts for the first time. A total maximum hydrogen demand potential of 108.9 Mt H_2/yr is identified considering industrial layouts nowadays, which can be fed by 313 hydrogen hubs with the weighted-average levelized cost of 1.26 – 4.53 USD/kg H_2 in 2060. Furthermore, a top-level strategy for scaling up shared hydrogen infrasturcture networks is envisaged built upon the multi-criteria and multi-scale comparison of these hydrogen hubs, which may provide insights into the design of policy instruments tailored to specific hydrogen hubs.

Keywords Green hydrogen, hard-to-abate industries, supply, end-use

JEL Classification D24, Q21, Q41, Q42

Contact tht20@mails.tsinghua.edu.cn
Publication May 2024
Financial Support Tsinghua Scholarship for Overseas Graduate Studies, Grant No. 2023123

Assessing China's green hydrogen supply and end-use diffusion in hard-to-abate industries

Haotian Tang[1, 2], David M. Reiner[2], Wenying Chen[1, *]

[1]Institute of Energy, Environment and Economy, Tsinghua University, Beijing 100084, China

[2]Judge Business School, University of Cambridge, Cambridge CB2 1AG, UK

[*]Correspondence: chenwy@tsinghua.edu.cn

Abstract

The deep decarbonization of China's hard-to-abate industries requires urgent expansion of clean hydrogen deployment, which is still in its infancy ascribed to its weak cost-competitiveness compared with the fossil-based counterparts and uncertain diffusion prospects. To address this problem, this study evaluates the supply potential and levelized cost of hydrogen production from onshore wind and solar PV on a 1 km-grid level, which collaborates with the established bottom-up plant-level hydrogen demand inventory to reveal the spatial heterogeneity and sectoral disparity of the hydrogen layouts for the first time. A total maximum hydrogen demand potential of 108.9 Mt H_2/yr is identified considering industrial layouts nowadays, which can be fed by 313 hydrogen hubs with the weighted-average levelized cost of 1.26 – 4.53 USD/kg H_2 in 2060. Furthermore, a top-level strategy for scaling up shared hydrogen infrasturcture networks is envisaged built upon the multi-criteria and multi-scale comparison of these hydrogen hubs, which may provide insights into the design of policy instruments tailored to specific hydrogen hubs.

1. Introduction

As an inevitable part of the investment portfolio underpinned by China's energy transition, hydrogen can be produced by various kinds of technologies combined with multiple sources of primary energy resources. Relying on the varying degrees of their respective carbon footprints, all the production routes can be further categorized into four major types: (1) the brown and grey hydrogen, which are produced from unabated fossil fuel, including the coal (through coal gasification combined with water-gas shift reaction), natural gas (through steam methane reforming) and other byproducts of industrial process[1]; (2) the blue hydrogen, which is based on the integration of carbon capture, utilization and storage (CCUS) into the industrial process of grey hydrogen to make it less carbon-intensive[2]; (3) the green hydrogen, which is based on the water electrolysis using carbon-neutral electricity or through biomass gasification coupled with CCUS, thus making the hydrogen carbon-neutral or even carbon-negative[3,4]; (4) the purple hydrogen, which takes advantages of the nuclear power and/or high-temperature heat to achieve water splitting[5]. Particularly, the green hydrogen based on water electrolysis using rebewable electricity has been

receiving rapidly growing attention in China, where the installed capacity is estimated to reach 50% of global capacity by the end of 2023[6]. However, clean hydrogen deployment still lags far behind the level required by net-zero emissions, mainly hampered by both the cost challenges of the above low-emission hydrogen-producing techonogies and highly uncertain hydrogen demand in new applications[7].

Nowadays, the vast majority of hydrogen is consumed in traditional applications including refining, ammonia synthesis for agricultural fertilizer and methanol preparation for high value-added chemicals, yet dominated by grey hydrogen[8]. Low-emission hydrogen's diffusion in the above industries and emerging applications, including hydrogen-based direct reduction of iron ore[9], hydrogen co-firing in industrial high-temperature kilns[10] and hydrogen-derived fuel production for hard-to-electrify transport[11], is still in an early stage and urgently requires policy supports to stimulate demand creation. Based on a few existing modeled energy transition pathways towards China's carbon neutrality, a deployment prospect of about 70 – 130 Mt H_2/yr is expected to be achieved in 2060, of which electrolytic hydrogen based on renewables account for 70% – 89.5%[7,11-14]. Such a significant uncertainty mainly resulting from different assumptions of technology competition in each sector may further leads to the hesitation in boosting the investment for scaling up pivotal infrastructures.

Considering these two problems in supply and demand side, it is of vital importance to conduct a spatially-explicit techono-economic analysis of China's green hydrogen supply and a bottom-up facility-level assessment of China's hydrogen end-use diffusion, thus laying a solid foundation for the design of support measures tailored to different regions and sectors. On the one hand, most existing research focus on the cost-competitiveness evaluation based on the calculation of the levelized cost of hydrogen production on a national or provincial scale[15], which fail to fully characterize the intraprovincial heterogeneity of economic viability contigent upon the land-use availability and the performance of variable renewable energy. On the other hand, the highly uncertain hydrogen demand projected by integrated assessment models[14,16,17], which usually presents as an aggregate for the whole sector within a large area, can't provide regionalized strategies due to the lack of asset-level techno-economic attributes, thereby sometimes underestimating or overestimating the hydrogen deployment potential to a certain extent.

To bridge the research gaps discussed above, first of all, this research implements techno-economic assessment on the technical potential and the levelized cost of electrolytic hydrogen production based on onshore wind and solar PV with a high resolution of 1 km, taking land suitability criteria, socio-economic and environmental filters, various kinds of technology combinations, and cost reduction potential into account. Then, this research establishes a bottom-up plant-level inventory of hydrogen demand potential based on collected information of 2038 industrial plants, covering the ironmaking and steelmaking, cement manufacturing, ammonia synthesis, methanol production, refining, coal-to-liquids, coal-to-gas, coal-to-olefins and coal-to-

ethylene glycol. Making the most of the insights obtained from the former analysis, a multi-scale and multi-cretiria characterization of heterogeneity in the identified 313 hydrogen hubs (i.e., hydrogen supply centers and hydrogen demand centers) is further carried out according to the derived levelized cost of hydrogen production and self-sufficiency indicators, which finally contributes to determining the early opportunities for hydrogen applications and conceiving the top-level strategies to promote large-scale hydrogen diffusion.

2. Methodology

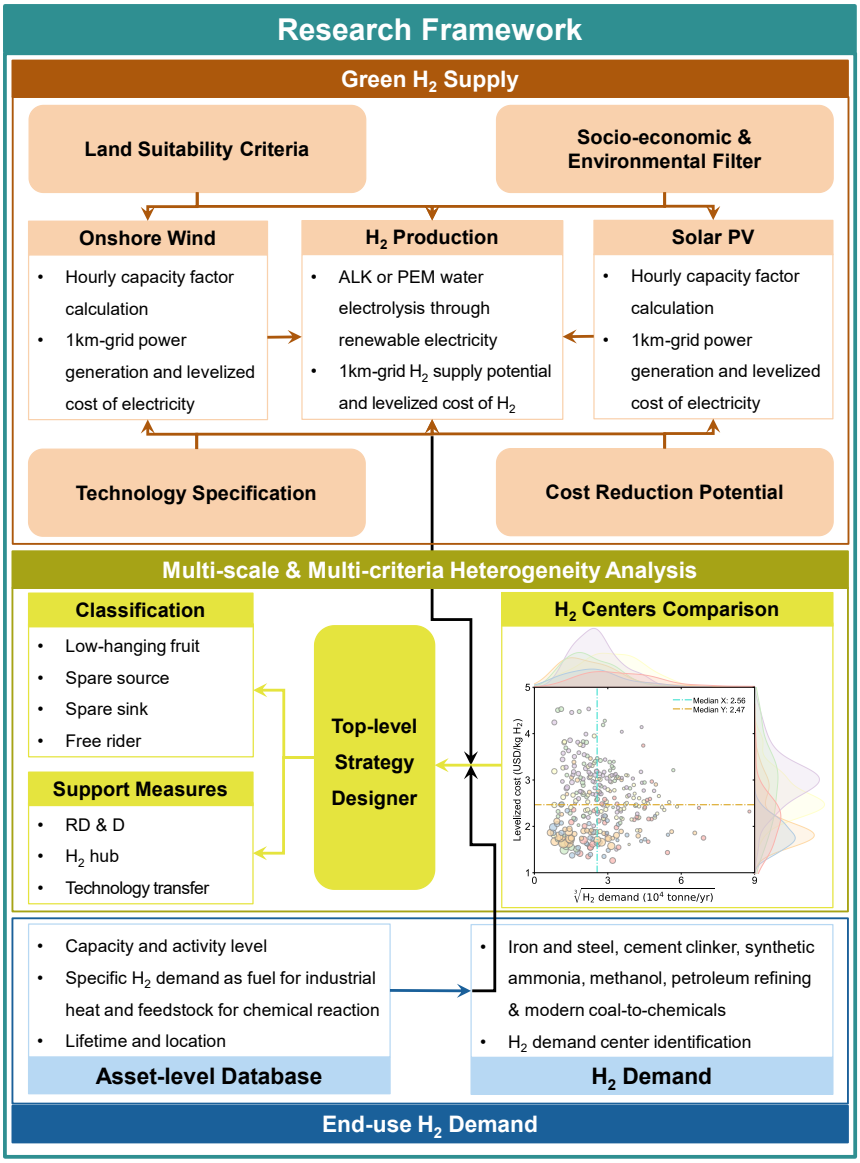

Figure 1. The research framework developed by this study. The brown, green and blue arrows represent the intra-module linkages, while the black arrows show the inter-module linkage of this framework.

This research develops a high-resolution and technology-explicit research framework to explore the layouts of green hydrogen supply potential and demand prospects aiming at China's

hard-to-abate industries for the first time (see **Figure 1**). To characterize the spatial heterogeneity and sectoral disparity of the hydrogen supply-demand layouts, this study employs spatially explicit techno-economic analysis of hydrogen production and facility-level assessment of hydrogen end-use diffusion, which are further integrated with a multi-scale and multi-criterion comparison of 313 identified hydrogen hubs, to propose top-level design of strategies for scaling up shared hydrogen infrastructure networks in China's energy system.

2.1 Green hydrogen techno-economic potential assessment

Taking advantage of multiple high-resolution geospatial data and technology-specific parameters, the Green H_2 Supply Module evaluates technical potential and levelized cost of hydrogen produced from various kinds of combinations of renewable resources and technologies on a 1km-grid level, with land-use related regulations, ecological and environmental protection, socio-economic factors and cost decline trends due to technological learning taken into account. The main criteria used to conduct land suitability analysis of this research are listed in **Table 1**.

Table 1. The main criteria used to conduct land suitability analysis[18-20].

Criterion	Category	Onshore wind	PV
Land cover	Croplands	0.25	0
	Forests	0.2	0
	Shrublands	0.2	0.05
	High & medium coverage grasslands	0.8	0
	Low coverage grasslands	0.8	0.8
	Water bodies	0	0
	Urban and built-up lands	0	0.05
	Barren	1	1
Slop (α for onshore wind and β for PV)	$0 \le \alpha \le 3\%,\ 0 \le \beta \le 5\%$	1	1
	$3\% < \alpha \le 6\%,\ \beta > 5\%$	0.5	0
	$6\% < \alpha \le 30\%$	0.3	–
	$30\% < \alpha$	0	–
Elevation (H)	$H \le 3000$m	1	–
	$H > 3000$m	0	–
Reserves	Ecologically functional zones	0	0
	Natural protected areas	0	0

More specifically, the land cover[21] and the elevation data[22] obtained from RESDC, both with a resolution of 1km, are used to determine suitable areas in view of land-use constraints and terrain obstacles and further evaluate capacity potential for renewable energy technology installation. Besides, ecologically functional zones[23], natural protected areas[24] and extremely resource-poor regions are eliminated from the candidate grid cells, on which the calculation of the technical

potential and levelized cost of hydrogen production via each technology route are based. The approaches to assess each renewable energy potential are detailed in section 2.1.1 and section 2.1.2.

2.1.1 Onshore wind power

To conduct hourly assessment of wind power capacity factor, wind speed fields with a spatial resolution of 0.25° longitude-latitude and a temporal resolution of 1 hour are retrieved from ERA5 reanalysis[25] and extrapolated to hub height assuming a vertical power law profile[26]:

$$\frac{v_h}{v_H} = \left(\frac{h}{h_H}\right)^{\alpha} \tag{1}$$

where v_h and v_H are hourly wind speed at hub height and the reference height of 100 m, respectively; h and h_H are wind turbine hub height and reference height of 100 m, respectively; α indicates the friction coefficient of $1/7$ adopted in this study. The derived wind speed fields at hub height are adjusted for air density to further calculate hourly wind power capacity factors using an approximate piece-wise power curve[27]:

$$cf_n^{wt} = \begin{cases} 0, & v_h < v_{cut-in} \\ \frac{v_h^3 - v_{cut-in}^3}{v_r^3 - v_{cut-in}^3}, & v_{cut-in} \le v_h < v_r \\ 1, & v_r \le v_h < v_{cut-out} \\ 0, & v_h \ge v_{cut-out} \end{cases} \tag{2}$$

where cf_n^{wt} indicates the hourly capacity factors; v_{cut-in}, v_r and $v_{cut-out}$ represent the cut-in, rated and cut-out wind speed according to the wind turbine specification.

The capacity installation and the electricity generation potential for onshore wind turbines are thereby estimated as Equation (3) and Equation (4), respectively:

$$C_n^{wt} = \frac{P_r^{wt}}{3D \times 10D} \cdot A_n \cdot s_n \tag{3}$$

$$E_n^{wt} = C_n^{wt} \cdot 8760 \cdot \overline{cf_n^{wt}} \tag{4}$$

where C_n^{wt} and E_n^{wt} are capacity installation (MW) and annual wind power generation (MWh/yr) of the n-th grid cell, respectively; P_r^{wt} is the rated power of a single onshore wind turbine considered in this research; D is the rotor diameter (m) of the wind turbine; $3D \times 10D$ represents the required wind turbine spacing[18]; A_n and s_n are the total area and assigned suitability factor of the n-th grid cell, respectively; $\overline{cf_n^{wt}}$ is the multi-annual average capacity factor spanning from 2018 to 2020.

2.1.2 Solar PV power

To characterize hourly performance of solar power generation, solar radiation data with a spatial resolution of 0.25° longitude-latitude and a temporal resolution of 1 hour are retrieved from ERA5 reanalysis[25] to derive hourly capacity factors, which are further corrected with temperature and shading coefficients[28-30]:

$$I_{panel} = (\cot\beta \cos\varphi \sin\sum + \cos\sum) \cdot I_{BH} + \frac{1+\cos\sum}{2} \cdot I_{DH} + \frac{1-\cos\sum}{2} \cdot \rho \cdot I_H \tag{5}$$

$$T_{cell} = T_{air} + \left(\frac{NOCT-20}{0.8}\right) \cdot I_{panel} \quad (6)$$

$$TEM = 1 + \delta \cdot (T_{cell} - 25) \quad (7)$$

$$\beta_{tmp} = \tan^{-1}\left(\frac{\tan\beta}{\cos\varphi_s}\right) \quad (8)$$

$$SHD = \left(\sin\sum\cot\beta\cos\varphi - \frac{\sin\sum}{\tan\beta_n}\cos\varphi_s\right) \cdot \frac{\sin\beta_{tmp}}{\sin(\pi-\beta_{tmp}-\sum)} \quad (9)$$

$$SHF = 1 - \left[floor\left(SHD \div \frac{1}{12}\right) + 1\right] \times \frac{1}{12} \quad (10)$$

$$cf^{pv} = \frac{I_{panel}}{I_0} \cdot TEM \cdot SHF \cdot \eta_{SYS} \quad (11)$$

where I_{panel}, I_{BH}, I_{DH} and I_H are hourly radiation intercepted by the PV panel (all in kW/m^2), direct beam radiation, diffuse radiation and the radiation reaching the horizontal surface for a certain grid cell, respectively; β, φ and $\sum$ symbolize solar altitude, solar azimuth and the optimum tilt of PV panel, respectively; β_n and φ_s signify solar altitude and solar azimuth at 3 PM on the day of winter solstice, respectively; T_{cell}, T_{air} and TEM indicate cell temperature (°C), ambient temperature (°C) and temperature correction coefficient, respectively; *NOCT* is the nominal operating cell temperature of 44 °C, with ambient temperature of 20 °C and solar irradiation of 0.8 kW/m^2; δ is the temperature coefficient of $-0.41\%/°C$; ρ, SHF, I_0 and η_{SYS} represent surface reflectance (0.2), shading coefficient, 1-sun of insolation (1 kW/m^2) and system efficiency (80.56%[29]), respectively; cf^{pv} denotes hourly solar power capacity factors for a certain grid cell.

Based on a linear fit proposed by Lu et al. [31], the optimum tilt (denoted as $\sum$) of PV panel at different latitudes (denoted as θ) is calculated as Equation (12):

$$\sum = \begin{cases} \theta, & 0° < \theta < 15°N \\ 1.1929 \times \theta - 11.79458, & \theta \geq 15°N \end{cases} \quad (12)$$

Therefore, the space-varying capacity installation (denoted as C^{pv}, MW) and hourly electricity generation potential (denoted as E^{pv}, MWh/yr) of solar PV for each grid cell are further estimated as:

$$PF = \frac{1}{\cos\sum + \frac{\sin\sum}{\tan\beta_n}\cos\varphi_s} \quad (13)$$

$$C^{pv} = PF \cdot P_0^{pv} \cdot A \cdot s \quad (14)$$

$$E^{pv} = C^{pv} \cdot 8760 \cdot \overline{cf^{pv}} \quad (15)$$

where PF indicates the ratio of effective panel area to the area of grid cells with PV installation; P_0^{pv} is the peak power of PV panels (161.9 MW/km^2 [29]); $\overline{cf^{pv}}$ is the multi-annual average capacity factor spanning from 2018 to 2020.

2.2 Green hydrogen supply potential and levelized production cost

For the above two renewable resources, water electrolysis with alkaline electrolyzer (ALK) and proton-exchange membrane electrolyzer (PEM) are considered as the technology routes to

further examine the technical potential and levelized cost of green hydrogen production. Specifically, the technical potential and the levelized cost of green hydrogen production based on water electrolysis are calculated as follows.

$$M_{n,t}^{i} = \frac{E_n^i \cdot \eta_t^{H_2}}{q^{H_2}}, i \in \{solar, PV\}, t \in \{ALK, PEM\} \quad (16)$$

$$LCOH_{n,t}^{i} = \frac{CAPEX_t^{H_2} \cdot CRF_t^{H_2} \cdot C_n^i + OPEX_t^{H_2} \cdot C_n^i + LCOE_n^i \cdot E_n^i}{M_{n,t}^i}, i \in \{solar, PV\}, t \in \{ALK, PEM\} \quad (17)$$

$$LCOE_n^i = \frac{CAPEX^i \cdot CRF^i \cdot C_n^i + OPEX^i \cdot C_n^i}{E_n^i}, i \in \{solar, PV\} \quad (18)$$

$$CRF = \frac{(1+r)^n \cdot r}{(1+r)^n - 1} \quad (19)$$

where $i \in \{solar, PV\}$ and $t \in \{ALK, PEM\}$ are two sets defined by renewable energy sources and electrolyzer categories. q^{H_2} is the lower heating value of hydrogen; $\eta_t^{H_2}$ is the electricity-to-hydrogen efficiency (%); *LCOE* and *LCOH* denote levelized cost of electricity and hydrogen, respectively; *CRF* is the capital recovery factor derived from the discount rate and the project lifetime for a specific technology; *CAPEX* and *OPEX* are unit investment cost and unit operational & maintenance cost for installing a specific technology with a capacity of C_n^i. E_n^i is the electricity input to produce hydrogen with a mass of $M_{n,t}^i$. More details about these techno-economic parameters are listed in Table 2.

Notably, the economic viability of green hydrogen is expected to benefit from technology advancement, which is manifested as technology performance enhancement and cost decrease owing to learning-by-doing effects. To explore the reduction potential of levelized cost of green hydrogen production, this study exogenously parameterizes the techno-economic attributes of renewable generation and electrolyzer systems in 2030 and 2060 in light of the published projections of future cost decrease trend based on technology learning curve approach, which can be found in **Table 2**.

2.3 Plant-level screening and accounting of hydrogen diffusion prospect

Acting as both clean fuel alternative for high-temperature industrial heat and feedstock for chemical reaction, green hydrogen is regarded as an important and even indispensable element in the investment portfolio for decarbonizing China's hard-to-abate industries. To unveil a panorama of hydrogen diffusion prospect in the industry sector, this study establishes a plant-level hydrogen demand potential database with a wide coverage of 9 sectors inclusive of iron- and steel-making, cement clinker manufacturing, ammonia synthesis, petroleum refining, methanol production, coal-to-liquids, coal-to-gas, coal-to-olefins and coal-to-ethylene glycol, containing geospatial information and techno-economic attributes of 2038 industrial plants. The hydrogen demand potential for each industrial plant is thereby estimated as:

$$DMD_{i,j,p} = CAP_{i,j,p} \cdot AF_{i,j,p} \cdot \omega_{i,j,p} \quad (20)$$

where $DMD_{i,j,p}$, $CAP_{i,j,p}$, $AF_{i,j,p}$ and $\omega_{i,j,p}$ are the hydrogen demand potential, capacity, availability factor and specific hydrogen demand (kg H_2/t product) for the plant i in sector j of province p, respectively. More details about the end-use hydrogen technologies and the corresponding specific hydrogen consumption are listed in **Table 3**.

Table 2. Techno-economic parameters of renewable electricity generation and hydrogen production technologies.

Parameter	Time	Onshore wind[26,32]	Solar PV[31-33]	ALK[15,34]	PEM[15,34]
CAPEX (USD/kW)	Base	1103	580	300	1200
	2030	816	300	252	700
	2060	527	221	187	214
OPEX (% of CAPEX/yr)	All	2	1	2.5	2.5
Lifetime	Base	20 years	25 years	60000 hours	45000 hours
	2030	20 years	25 years	75000 hours	60000 hours
	2060	20 years	25 years	100000 hours	100000 hours
Efficiency (%)	Base	–	–	60	65
	2030	–	–	65	70
	2060	–	–	75	80
Discount rate (%)	All	8	8	8	8

Table 3. The specific hydrogen consumption of end-use hydrogen technologies considered in this research for different industries.

Industries	End-use H_2 technology	Ranges of specific H_2 demand (kg H_2/t product)	Assumed specific H_2 demand (kg H_2/t product)
Iron and steel	H_2-based direct reduction	51 – 81[35-38]	60
Cement	H_2-cofiring in cement kilns	2.91 – 34.02[38,39]	11
Ammonia	Haber-Bosch process	179.4 – 204[38,40-42]	204
Methanol	$CO + 2H_2 \rightarrow CH_3OH$	128 – 525[17,38,41,43,44]	190
Refinery	Hydrotreatment and hydrocracking	14.6 – 18[6,38,45]	14.6
Direct coal-to-liquids	$nC + (n+1)H_2 \rightarrow C_nH_{2n+2}$	–	190[41]
Indirect coal-to-liquids	$nCO + (2n+1)H_2 \rightarrow C_nH_{2n+2} + nH_2O$	–	313[41]
Coal-to-gas	$CO + 3H_2 \rightarrow CH_4 + H_2O$	–	311[41]
Coal-to-olefins	$CO + 2H_2 \rightarrow CH_3OH$, $nCH_3OH \rightarrow C_nH_{2n} + nH_2O$	–	417[41]
Coal-to-ethylene glycol	$2CO + 4H_2 + 0.5O_2 \rightarrow C_2H_4(OH)_2 + H_2O$	–	266[41]

3. Results and discussion

3.1 China's technical potential of green hydrogen supply

As seen from **Figure 2A and 2B**, the technical potential of green hydrogen is inclined to be much more abundant in northern and western regions of China than in southern and eastern counterparts. For the gross technical potential of 4.3 Gt H_2/yr identified in this study, the onshore wind and solar PV register about 9% and 91% of the total, respectively. The differing technical potential between two electricity-generating H_2-producing routes could be explained by different land-use intensity of wind turbines and PV panels, though fairly contingent upon ever-evolving land acquisition policies and assumed suitability indicators for various land cover. Furthermore, huge disparities of green hydrogen potential also present among provinces, with Inner Mongolia and Xinjiang altogether accounting for about 72% and 58% of the total hydrogen produced from wind and solar energy, respectively.

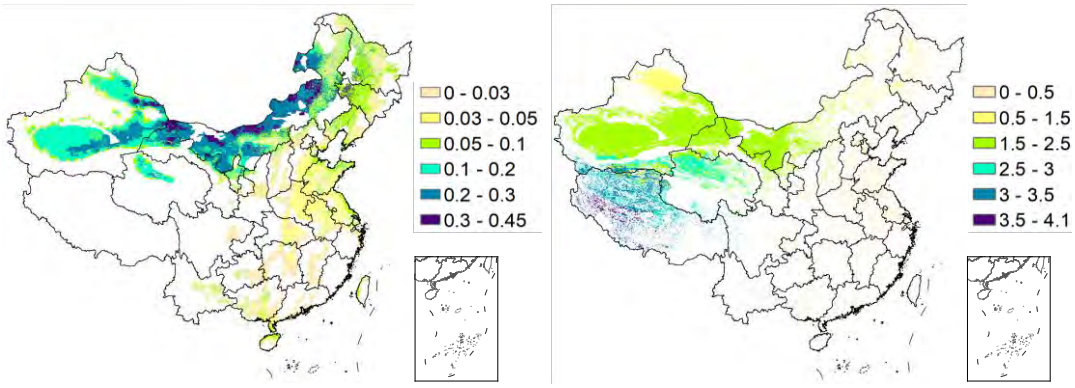

Figure 2. The technical potential of green hydrogen based on PEM electrolyzers in 2060. (A) and (B) – 1 km-grid distribution for green hydrogen produced from onshore wind and solar PV, respectively.

Additionally, the green hydrogen generated from solar show a more concentrated distribution than the counterpart from wind, which is indicated by the ratios of gross area of the top five provinces to the total area of all sectors in **Figure 3A and 3B**. Specifically, the top five provinces contribute around 97% and 86% of the total technical potential for green hydrogen based on solar and wind, respectively. While some provinces of North China and Northwest China are rich in both wind and solar energy resources, Heilongjiang, Jilin and Liaoning of Northeast China may witness comparative advantages in wind-based hydrogen supply, as their aggregate share of the total wind energy is almost 10 times their aggregate share of the total solar energy. However, some regions of Southwest China and South-Central China are considerably poor in both wind and solar resources and may have to seek other renewable generation technologies like hydropower or thermo-chemical conversion pathways like biomass gasification.

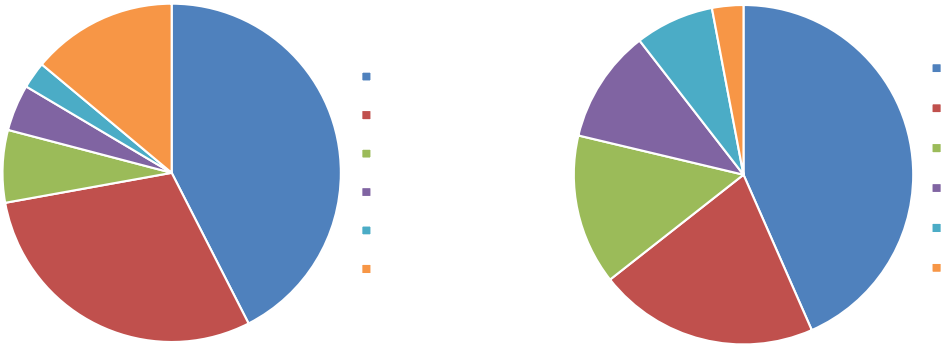

Figure 3. Provincial-level aggregation of green hydrogen potential. (A) and (B) – The provincial-level shares in green hydrogen produced from onshore wind and solar PV, respectively. Please note that the top five provinces with green hydrogen potential are listed separately, while the rest are aggregated into one item in each pie chart.

3.2 Economic viability of green hydrogen via different technology routes

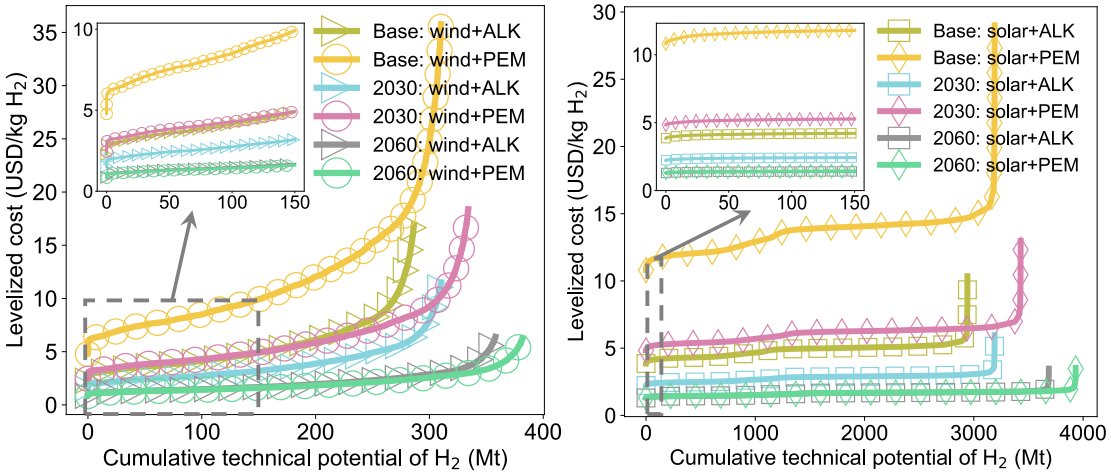

Figure 4. Levelized production cost of green hydrogen. (A) and (B) –The reduction potential for levelized cost of green hydrogen production via different routes based on onshore wind and solar PV, respectively.

The levelized cost reduction potential is of vital importance for the techno-economic competitiveness of green hydrogen diffusion in end-use sectors. As most recently published research suggest a hydrogen demand prospect of around 70 – 130 Mt H_2/yr in 2060 required by China's carbon neutrality vision, an upper limit of 150 Mt H_2/yr is further imposed on the levelized cost curves in **Figure 4A and 4B** to amplify the cost variations within that relative small range. Currently, renewable generation coupled with ALK electrolyzer performs better than with PEM electrolyzer

in terms of the economic viability, with the weighted-average levelized cost of about 3.9 – 4.1 USD/kg H_2 and 8.0 – 11.6 USD/kg H_2 for ALK and PEM to meet the upper demand prospect of 150 Mt H_2/yr, respectively. Furthermore, the weighted-average levelized cost for ALK-based routes, below the supply potential of 150 Mt H_2/yr, is likely to reach about 2.48 USD/kg H_2 in 2030 and even 1.39 USD/kg H_2 in 2060. However, PEM-based green hydrogen would witness a remarkable increase in cost-competitiveness boosted by the combination of technology learning and technology performance advancement, which decreases to 4.05 – 5.18 USD/kg H_2 in 2030 and about 1.35 – 1.40 USD/kg H_2 in 2060, finally reaching cost parity compared with the ALK-based routes. The cost dynamics identified in this assessment largely mirrors the cost range reported in previous research focusing on the national level[4,15], thus demonstrating the validity of this study to some extent, and further provides more details for sub-regional disparity.

3.3 China's end-use hydrogen diffusion prospect based on current industrial layouts

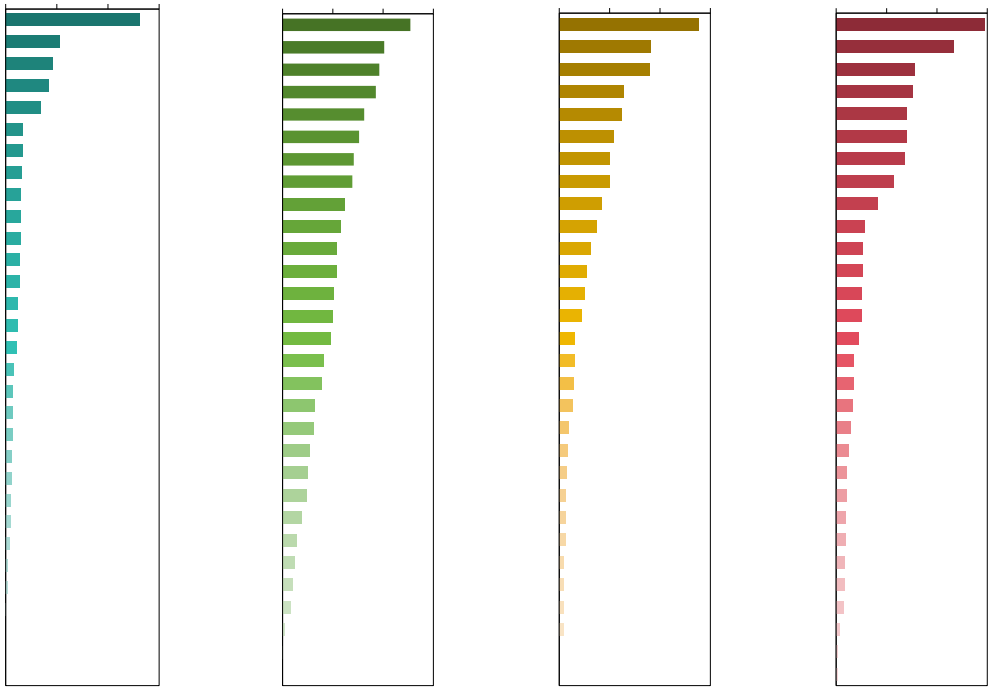

Figure 5. Provincial-level aggregation of sectoral hydrogen demand potential. (A) –the iron and steel industry; (B) – the cement industry; (C) – the ammonia and the methanol industry; (D) – the petroleum refining industry and the modern coal-to-chemical industry (MCCI). Please note that among China's 34 provincial-level administrative regions, Xizang, Hongkong, Macao and Taiwan are not assessed in this section due to the limit of data availability.

Acting as alternative fuel for high-temperature heat and the feedstock for chemical reactions in industrial process, clean hydrogen is regarded as an important leverage for the decarbonization

of difficult-to-electrify activities especially in hard-to-abate industries. Among the total maximum hydrogen demand potential of 108.9 Mt H_2/yr analyzed in this study, the ironmaking and steelmaking ranks first with a potential of about 52.6 Mt H_2/yr. Next comes the cement manufacturing, accounting for 15.2% of the total potential. The remaining potential of 39.7 Mt H_2/yr is contributed by ammonia synthesis, methanol production, refineries and modern coal-to-chemicals, comprising 9.7%, 13.5%, 9.1% and 4.2% of the total potential of 108.9 Mt H_2/yr, respectively.

At present, traditional fossil fuel-based steel manufacturing routes, namely blast furnace ironmaking-basic oxygen furnace steelmaking (BF-BOF) comprises nearly 90% of the total annual output of crude steel in China. Given the current layouts of China's iron and steel industry and the technology performance of hydrogen-based direct reduction of iron (H_2-DRI), the hydrogen deployment prospect for the iron and steel industry is evaluated and shown in **Figure 5A**. Notably, the hydrogen deployment prospect would reach over 20% of the total sectoral potential in Hebei Province alone, with all the existing capacity transformed into the H_2-DRI route. Specifically, the top five provinces with crude steel production capacity would donate about 58% of the total sectoral hydrogen demand potential, implying a rather concentrated industrial layout. Considering hydrogen as a fuel substitution in clinker production, the hydrogen diffusion potential in cement manufacturing is examined and illustrated in **Figure 5B**. The top five provinces with cement clinker production capacity make up only 36% of the total sectoral potential, suggesting a more distributed industrial layout compared to the iron and steel industry. The above two sectors are expected to become brand-new end-use applications for China's hydrogen scaling-up, while the traditional and modern coal chemical industry and petroleum refining consume the vast majority of hydrogen nowadays, which will continue to play an indispensable role in the future. As depicted in **Figure 5C and 5D**, some provinces of North China, East China and Northwest China may have a larger potential for end-use hydrogen applications, which are driven by the combination of regional resource endowment and socio-economic demand. For instance, Inner Mongolia, Shandong and Shaanxi, all with considerable hydrogen deployment prospects, are anticipated to register a potential of about 4.9, 4.6 and 3.3 Mt H_2/yr for these four industries, respectively.

These 2038 industrial plants are further spatially aggregated into 313 hydrogen end-use demand centers, which are contingent upon the conversion of individual polygons for each administrative regions to corresponding point features. As seen from **Figure 6A**, the major hydrogen demand centers with a prospect of exceeding 1 Mt H_2/yr mainly lie in Hebei, Inner Mongolia, Shandong, Shanxi, Shaanxi, Ningxia, Jiangsu and Liaoning. Specifically, Tangshan (in Hebei Province), Ordos (in Inner Mongolia Autonomous Region), and Handan (in Hebei Province) are the top three cities in terms of hydrogen diffusion potential, reaching 6.8, 3.3, and 3.0 Mt H_2/yr, respectively. While the hydrogen deployment prospect in Tangshan and Handan are largely attributable to their iron and steel industry, the counterpart in Ordos is mainly contributed by its coal chemical industry. Such a remarkable disparity in regional industrial structure is further revealed in

Figure 6B. Unlike East China's relatively balanced shares for various kinds of hard-to-abate industries, other regions tend to be particularly outstanding or weak in specific categories. For example, North China makes up about 36% of the total hydrogen end-use applications for the overall iron and steel industry, with a share of only 7.6% in the overall cement industry. However, a completely opposite pattern is identified for Southwest China, with a share of 6.5% and 23.5% in the overall iron and steel industry and the cement industry, respectively. Moreover, Northwest China accounts for about 23.8% of the total hydrogen deployment prospect in the overall chemical industry (namely methanol, ammonia, refinery and modern coal-to-chemicals in this study), yet with a much humble proportion of 4.1% and 8.8% for the overall iron and steel industry and the cement industry, respectively.

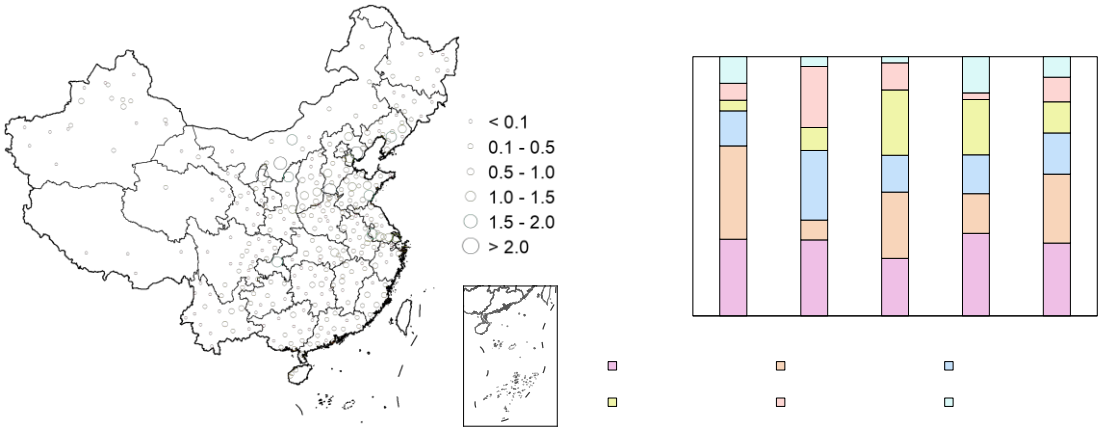

Figure 6. China's hydrogen end-use diffusion prospect based on current industrial layouts. (A) – the identified promising hydrogen demand centers; (B) – Regional shares in the total hydrogen demand prospect for each industry. Note that ISI – iron and steel; CEM – cement; MeOH – methanol; NH_3 – ammonia; REN – refinery; MCCI – modern coal-to-chemical industry.

3.4 Top-level design of strategies for scaling up shared hydrogen infrastructure networks

Taking advantage of the techno-economic analysis of prospective hydrogen hubs on both supply and demand side, this study reveals a panorama of the spatial heterogeneity of resource potential and economic-viability, which is conducive to designing the top-level strategies of hydrogen deployment in a more targeted manner. As shown in Figure 7A, four quadrants (denoted as *Q I*, *Q II*, *Q III*, and *Q IV*) are defined by two axes signifying the median levelized cost of green hydrogen production and the median cube root of hydrogen demand potential. According to the horizontal and vertical coordinates of individual bubble points, the corresponding hydrogen hubs are classified into four different roles in Figure 7B. The lower the levelized cost is, the stronger supply-side competitiveness the corresponding administrative region will exhibit; the larger the hydrogen demand potential, the more demand-side benefits owing to economies of scale the

corresponding administrative region will get.

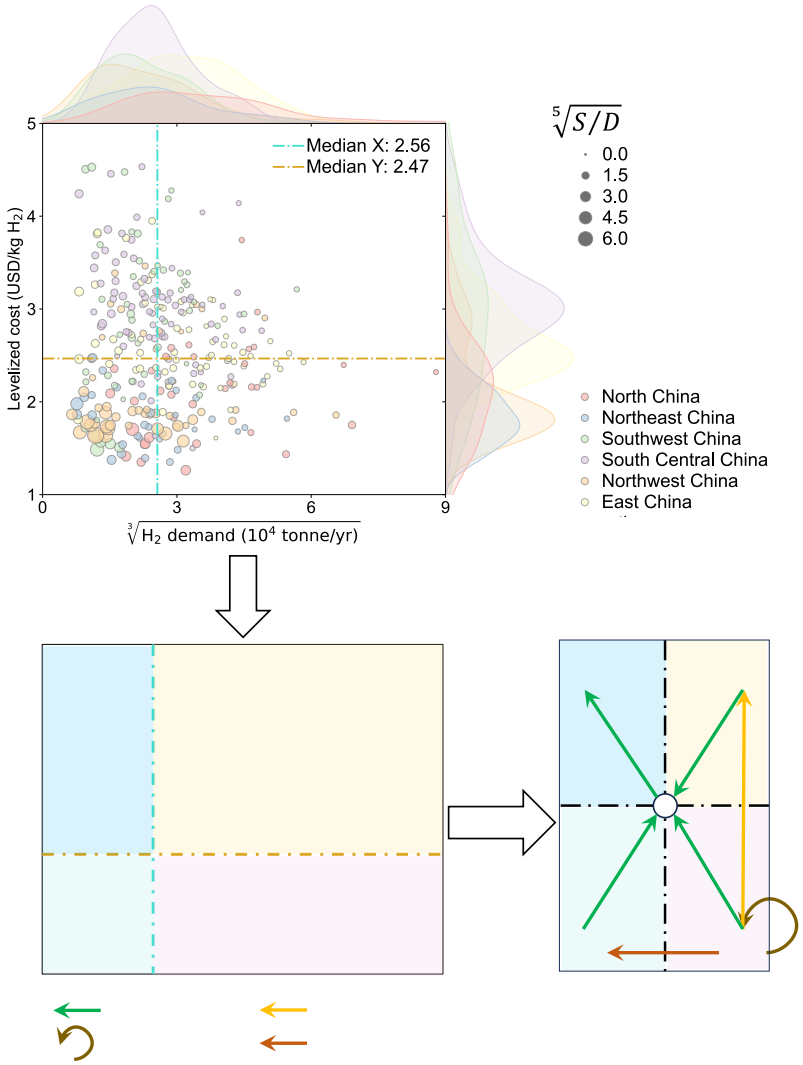

Figure 7. Top-level design of hydrogen deployment strategies based on multi-dimensional characterization of prospective hydrogen supply/demand centers. (A) – Multi-level and multi-criteria analysis of hydrogen supply/demand centers; (B) – The classification of hydrogen supply/demand centers according to individual supply/demand potential and cost-competitiveness; (C) A proposed top-level strategy for scaling up shared hydrogen infrastructure networks. Note that S/D represents $supply\ potential/demand\ potential$.

Based on the above techno-economic attributes depicted in **Figure 7A** and the identified roles in **Figure 7B**, regional-specific and top-level strategies for promoting hydrogen deployment are proposed in **Figure 7C**. Those who simultaneously have a lower levelized cost and a larger hydrogen demand prospect can be regarded as low-hanging fruits, thus favoring early batches of research, development and demonstration (RD & D) and even boosting large-scale hydrogen

deployment in other areas based on customized technology transfer. Furthermore, a complementary techno-economic feature exists between the administrative regions of *Q I* and *Q III*. As the hydrogen deployment gradually increases, the supply-demand equilibrium supported by *Q IV* alone could be broken, thereby requiring the involvement of spare sources and spare sinks in *Q III* and *Q I*, respectively. However, neither of these advantages presents in the administrative regions of *Q II*. One possible way to enable clean hydrogen diffusion in that category is to make the most of the economies of scale by establishing a large-scale hydrogen infrastructure network, which consists of multiple hydrogen supply or demand hubs connected by shared transport corridors.

4. Conclusion and policy implications

This research conducts spatially explicit bottom-up assessment of China's techno-economic potential of green hydrogen supply and explore promising hydrogen end-use diffusion layouts in the hard-to-abate sectors by collecting relevant information of 2038 industrial plants. Results show that a total technical potential of 4.3 Gt H_2/yr is identified in this research, which is far more than the prospects of 70 – 130 Mt H_2/yr projected by series of modeled energy transition pathways towards China's carbon neutrality. Furthermore, the economic viability of green hydrogen supply would witness a remarkable improvement, with the weighted-average levelized cost expected to reach 1.35 – 1.40 USD/kg H_2 in 2060. For some areas which are extremely good in renewable resource performance, the minimum levelized cost can be even below 1 USD/kg H_2. Among all the 313 demand centers recognized by this research, 24 large-scale demand hubs, each with a prospect of over 1 Mt H_2/yr, comprise nearly 40% of the total demand potential of 108.9 Mt H_2/yr, and exhibit diverse patterns of hydrogen end-use applications due to distinct industrial structures.

Considering varying degrees of cost-competitiveness and different scales of supply or demand capacity, a top-level strategy for boosting hydrogen deployment in hard-to-abate sectors is proposed. Firstly, more early batches of RD & D should be encouraged in the regions classified as "low-hanging fruits" to enable effective technology learning and performance advancement. Next, the technology transfer of hydrogen production and end-use is supposed to be promoted in an orderly and tailored manner. Taking the end-use application as an example, the large-scale iron and steel plants with low-cost green hydrogen sources can take the lead in RD & D of hydrogen-based shaft furnace direct reduction process and then share their management experience and technical specifications with the others. Finally, shared hydrogen pipeline should be constructed to connect those large-scale hydrogen hubs, namely hydrogen supply centers and demand centers. Most importantly, this may provide an opportunity for those relatively small industrial plants to join the shared infrastructure networks.

Reference

1 IEA. The Future of Hydrogen. (Paris, 2019).

2 IEA. Opportunities for Hydrogen Production with CCUS in China. (Paris, 2022).

3 Matthias Binder, M. K., Matthias Kuba, and Markus Luisser. Hydrogen from biomass gasification. IEA Bioenergy. (2018).

4 IRENA. Global hydrogen trade to meet the 1.5°C climate goal: Part III – Green hydrogen cost and potential. (Abu Dhabi, 2022).

5 Elizabeth Connelly, M. P., Anelia Milbrandt, Billy Roberts, Nicholas Gilroy, and Marc Melaina. Resource Assessment for Hydrogen Production. National Renewable Energy Laboratory. (Golden, 2020).

6 IEA. Global Hydrogen Review 2023. (Paris, 2023).

7 IEA. An energy sector roadmap to carbon neutrality in China. (Paris, 2021).

8 Shuyi Li, Yujun Xue, and Peishan Wang. Transforming China's Chemicals Industry: Pathways and Outlook under the Carbon Neutrality Goal. RMI. (2022).

9 Ji Chen, Shuyi Li, Xiangyi Li, Ye (Agnes) Li. Pursuing Zero-Carbon Steel in China: A Critical Pillar to Reach Carbon Neutrality. RMI. (2021).

10 RMI and China Cement Association. Toward Net Zero: Decarbonization Roadmap for China's Cement Industry. (2022).

11 Ting Li, Wei Liu. The key to a new era of green hydrogen energy: China's development roadmap for renewable hydrogen of 100 GW in 2030. RMI and China Hydrogen Alliance Research Institute. (2022).

12 PetroChina. World and China Energy Outlook 2060: The 2023 Edition. (Beijing, 2023).

13 Sinopec. China Energy Outlook 2060: The 2024 Edition. (Beijing, 2023).

14 Yang, X., Nielsen, C. P., Song, S. & McElroy, M. B. Breaking the hard-to-abate bottleneck in China's path to carbon neutrality with clean hydrogen. *Nature Energy* **7**, 955-965 (2022). https://doi.org:10.1038/s41560-022-01114-6

15 Wang Y Z, O. X. M., Zhou S. Future cost trend of hydrogen production in China based on learning curve. *Climate Change Research* **18**, 11 (2022). https://doi.org:10.12006/j.issn.1673-1719.2021.248

16 Shao, T., Pan, X., Li, X., Zhou, S., Zhang, S. & Chen, W. China's industrial decarbonization in the context of carbon neutrality: A sub-sectoral analysis based on integrated modelling. *Renewable and Sustainable Energy Reviews* **170**, 112992 (2022). https://doi.org:https://doi.org/10.1016/j.rser.2022.112992

17 Xiang, P.-P., He, C.-M., Chen, S., Jiang, W.-Y., Liu, J. & Jiang, K.-J. Role of hydrogen in China's energy transition towards carbon neutrality target: IPAC analysis. *Advances in Climate Change Research* **14**, 43-48 (2023). https://doi.org:https://doi.org/10.1016/j.accre.2022.12.004

18 Wang, Y., Chao, Q., Zhao, L. & Chang, R. Assessment of wind and photovoltaic power potential in China. *Carbon Neutrality* **1**, 15 (2022). https://doi.org:10.1007/s43979-022-00020-w

19 Wang, Y. *et al.* Accelerating the energy transition towards photovoltaic and wind in China. *Nature* **619**, 761-767 (2023). https://doi.org:10.1038/s41586-023-06180-8

20 Tian, J., Zhou, S. & Wang, Y. Assessing the technical and economic potential of wind and solar energy in China—A provincial-scale analysis. *Environmental Impact Assessment Review* **102**, 107161 (2023). https://doi.org:https://doi.org/10.1016/j.eiar.2023.107161

21 Xu, X. et al. China's multi-period land use land cover remote sensing monitoring dataset (CNLUCC). RESDC https://doi.org/10.12078/2018070201 (2018).

22 RESDC. The 1-km DEM data for China's elevation distribution. RESDC (2024).

23 RESDC. China's ecologically functional zones. RESDC (2024).

24 UNEP-WCMC and IUCN (2024), Protected Planet: The World Database on Protected Areas (WDPA) [Online], March 2024, Cambridge, UK: UNEP-WCMC and IUCN. Available at: www.protectedplanet.net..

25 Hersbach, H., Bell, B., Berrisford, P., Biavati, G., Horányi, A., Muñoz Sabater, J., Nicolas, J., Peubey, C., Radu, R., Rozum, I., Schepers, D., Simmons, A., Soci, C., Dee, D., Thépaut, J-N. (2023): ERA5 hourly data on single levels from 1940 to present. Copernicus Climate Change Service (C3S) Climate Data Store (CDS), DOI: 10.24381/cds.adbb2d47 (Accessed on 17-Jan-2024).

26 Chen, S., Xiao, Y., Zhang, C., Lu, X., He, K. & Hao, J. Cost dynamics of onshore wind energy in the context of China's carbon neutrality target. *Environmental Science and Ecotechnology* **19**, 100323 (2024). https://doi.org:https://doi.org/10.1016/j.ese.2023.100323

27 Yu, S., Gui, H. & Yang, J. China's provincial wind power potential assessment and its potential contributions to the "dual carbon" targets. *Environmental Science and Pollution Research* **30**, 13094-13117 (2023). https://doi.org:10.1007/s11356-022-23021-9

28 Masters, G. M. *Renewable and Efficient Electric Power Systems*. (John Wiley & Sons, Inc., 2004).

29 Chen, S. *et al.* The Potential of Photovoltaics to Power the Belt and Road Initiative. *Joule* **3**, 1895-1912 (2019). https://doi.org:https://doi.org/10.1016/j.joule.2019.06.006

30 Qiu, T. *et al.* Potential assessment of photovoltaic power generation in China. *Renewable and Sustainable Energy Reviews* **154**, 111900 (2022). https://doi.org:https://doi.org/10.1016/j.rser.2021.111900

31 Lu, X. *et al.* Combined solar power and storage as cost-competitive and grid-compatible supply for China's future carbon-neutral electricity system. *Proceedings of the National Academy of Sciences* **118**, e2103471118 (2021). https://doi.org:doi:10.1073/pnas.2103471118

32 IRENA. Renewable power generation costs in 2022. (Abu Dhabi, 2023).

33 Zhang, D. *et al.* Spatially resolved land and grid model of carbon neutrality in China. *Proceedings of the National Academy of Sciences* **121**, e2306517121 (2024). https://doi.org:doi:10.1073/pnas.2306517121

34 Huang, J., Balcombe, P. & Feng, Z. Technical and economic analysis of different colours of producing hydrogen in China. *Fuel* **337**, 127227 (2023). https://doi.org:https://doi.org/10.1016/j.fuel.2022.127227

35 Vogl, V., Åhman, M. & Nilsson, L. J. Assessment of hydrogen direct reduction for fossil-free steelmaking. *Journal of Cleaner Production* **203**, 736-745 (2018). https://doi.org:https://doi.org/10.1016/j.jclepro.2018.08.279

36 Bhaskar, A., Abhishek, R., Assadi, M. & Somehesaraei, H. N. Decarbonizing primary steel production : Techno-economic assessment of a hydrogen based green steel production plant in Norway. *Journal of Cleaner Production* **350**, 131339 (2022). https://doi.org:https://doi.org/10.1016/j.jclepro.2022.131339

37 Benavides, K. *et al.* Mitigating emissions in the global steel industry: Representing CCS and hydrogen technologies in integrated assessment modeling. *International Journal of Greenhouse*

Gas Control **131**, 103963 (2024). https://doi.org:https://doi.org/10.1016/j.ijggc.2023.103963

38 Neuwirth, M., Fleiter, T., Manz, P. & Hofmann, R. The future potential hydrogen demand in energy-intensive industries - a site-specific approach applied to Germany. *Energy Conversion and Management* **252**, 115052 (2022). https://doi.org:https://doi.org/10.1016/j.enconman.2021.115052

39 Williams, F., Yang, A. & Nhuchhen, D. R. Decarbonisation pathways of the cement production process via hydrogen and oxy-combustion. *Energy Conversion and Management* **300**, 117931 (2024). https://doi.org:https://doi.org/10.1016/j.enconman.2023.117931

40 Fasihi, M., Weiss, R., Savolainen, J. & Breyer, C. Global potential of green ammonia based on hybrid PV-wind power plants. *Applied Energy* **294**, 116170 (2021). https://doi.org:https://doi.org/10.1016/j.apenergy.2020.116170

41 Guo, Y., Peng, L., Tian, J. & Mauzerall, D. L. Deploying green hydrogen to decarbonize China's coal chemical sector. *Nature Communications* **14**, 8104 (2023). https://doi.org:10.1038/s41467-023-43540-4

42 IRENA and AEA. Innovation Outlook: Renewable Ammonia. (Abu Dhabi and Brooklyn, 2022).

43 IRENA and METHANOL INSTITUTE. Innovation Outlook : Renewable Methanol. (Abu Dhabi, 2021).

44 Sarp, S., Gonzalez Hernandez, S., Chen, C. & Sheehan, S. W. Alcohol Production from Carbon Dioxide: Methanol as a Fuel and Chemical Feedstock. *Joule* **5**, 59-76 (2021). https://doi.org:https://doi.org/10.1016/j.joule.2020.11.005

45 Wang, M. Research on the development path of modern coal chemical industry coupled by green hydrogen. *China Coal* **49**, 102-107 (2023). https://doi.org:10.19880/j.cnki.ccm.2023.05.014